



HAL
open science

Modelling and analysis of vibrations on an aerial cable car system with moving mass

Cesar Augusto Fonseca, Guilherme Rodrigues Sampaio, Geraldo F de S Rebouças, Marcelo Pereira, Americo Cunha Jr

► **To cite this version:**

Cesar Augusto Fonseca, Guilherme Rodrigues Sampaio, Geraldo F de S Rebouças, Marcelo Pereira, Americo Cunha Jr. Modelling and analysis of vibrations on an aerial cable car system with moving mass. Second International Nonlinear Dynamics Conference, Feb 2021, Rome, Italy. hal-03130836v1

HAL Id: hal-03130836

<https://hal.science/hal-03130836v1>

Submitted on 3 Feb 2021 (v1), last revised 27 Apr 2021 (v2)

HAL is a multi-disciplinary open access archive for the deposit and dissemination of scientific research documents, whether they are published or not. The documents may come from teaching and research institutions in France or abroad, or from public or private research centers.

L'archive ouverte pluridisciplinaire **HAL**, est destinée au dépôt et à la diffusion de documents scientifiques de niveau recherche, publiés ou non, émanant des établissements d'enseignement et de recherche français ou étrangers, des laboratoires publics ou privés.

Copyright

Modelling and analysis of vibrations on an aerial cable car system with moving mass

Cesar Augusto Fonseca¹, Guilherme Rodrigues Sampaio², Geraldo F. de S. Rebouças³, Marcelo Pereira⁴, and Americo Cunha Jr⁴

¹ Centro de Instrução Almirante Wanderkolk – CIAW, Rio de Janeiro, Brazil
`cesar.linhares@marinha.mil.br`

² RIO Analytics, Rio de Janeiro, Brazil
`guirsp@gmail.com`

³ Norwegian University of Science and Technology – NTNU, Trondheim, Norway
`geraldo.reboucas@ntnu.no`

⁴ Rio de Janeiro State University – UERJ, Rio de Janeiro, Brazil
`marcelocpereira@globo.com`
`americo.cunha@uerj.br`

Abstract. The main purpose of this work is to study the nonlinear dynamics of an aerial cable car system. The mechanical system presented consists of two cables, a traction cable, and a supporting cable. The car is modeled as a concentrated mass pulled by a traction cable. The mathematical model is described as a mass-spring system attached to a time-varying length cable. The effects of the pulling speed shall generate nonlinear features due to the coupling between the cable and the car and due to external excitation.

Keywords: cable car system, nonlinear dynamics, moving boundary problem, time-scale separation

1 Introduction

The transport of people and goods over aerial cableways, as seen in Figure 1, has been in use over the last hundred years for many different applications. This type of transport is present in thousands of installations, Switzerland has alone more than 130 in operation. The study of cable car systems is an interesting subject in modern literature, with many different aspects of the system approached, but published works on this topic are still only a few years old. Since it is a complex mechanical system with many bodies, flexibility, and subject to environmental perturbations, nonlinear phenomena may appear such as excitation of sub and super harmonics on the cable causing vibration to the traction mechanism, which can damage the machinery and endanger the operation.

The mechanical system studied consists of two cables, a supporting cable fixed in both ends, and a variable-length traction cable. The car is modeled as a concentrated mass pulled by the traction cable and connected to the supporting cable through a spring. In this work, we analyze the effect of vibrations in the

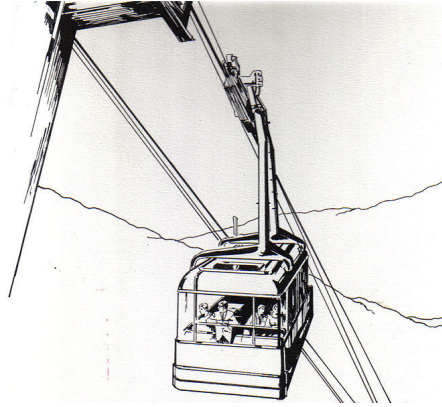


Fig. 1. Line art drawing of a typical aerial cable car system.

traction cable according to the speed of operation and position of the car. The coupling of the two cables and a mass-spring system creates a complex dynamic that causes a nonlinear movement and can even show some chaotic behavior. Some references found in the literature such as the modeling of elevators show resemblance to the present study.

The work of Brownjohn [1] analyses the vertical plane motion of the cable car that connects Singapore's main island and the island of Sentosa. Mathematical simulations are presented for the normal operation of the system, free vibration, and when the system is halted. Measurements with accelerometers were performed in the real system to obtain vibrations for each condition of operation. A finite element model of the system is then proposed and the results are analyzed.

Terumichi et. al. [2] studies the nonstationary lateral vibration of a string with time-varying length and a rail-guided mass-spring system attached at the lower end, a representative system of an elevator. The string is sinusoidally excited by a horizontal displacement at its upper end. The influence of the axial velocity of the string on the vibrations are analyzed and a simplified experimental setup is presented. Experimental and simulation results are then compared showing good agreement.

Bao et. al. [3] also analyzes lateral vibrations in a string in a vertical motion system analog to an elevator, but in this case, the source of excitation is the lateral motion of the mass coming from an imperfect rail guide. The Hamilton principle is used to obtain the equations of motion of the string, and experimental tests are performed and its results compared to the numerical simulations.

Finally, Kaczmarczyk and Iwankiewicz [4] propose a stochastic approach to the source of excitation of an elevator model, where the stochastic parameter is the guide rail imperfections that excite the car laterally. These imperfections are written as a zero-mean stationary Gaussian process. Although the model proposed in this work uses a strict deterministic approach, the knowledge on

time-scale separation shown is essential for solving the problem, as seen in another work of the same author [5].

Those works show that despite the presented cable vibration theories, there are still very few applications to aerial cable car systems, a common system around the world, where a failure can endanger many lives. Cable car systems differ significantly from elevators as the gravity acts transversely to the cable.

The main originality of this work is to develop a mechanical model of a cable car system, to investigate the influence of its parameters using numerical methods, and to explore some of its nonlinearities. The manuscript is organized as follows: the mechanical-mathematical model for the system of interest is presented in Section 2, the numerical results, and a brief discussion in Section 3, and finally the conclusions are made in Section 4.

2 Mechanical-mathematical model

The proposed mechanical system is illustrated in Figure 2, where a pair of overhung cables has a constant value of tension and is fixed on both ends with density, circular cross-section, and constant length. The purpose of this cable is to provide support to the cable car and to serve as the rails, where the cable car slides on. Later, the rail cables are simplified as a single spring K attached to the cable car represented by the concentrated mass M . The car is pulled by another cable with a linear density ρ , cross-section A , and tension T . However, the length of the traction cable varies in time with constant velocity v , pulling the mass M to the origin, where the pulley is located.

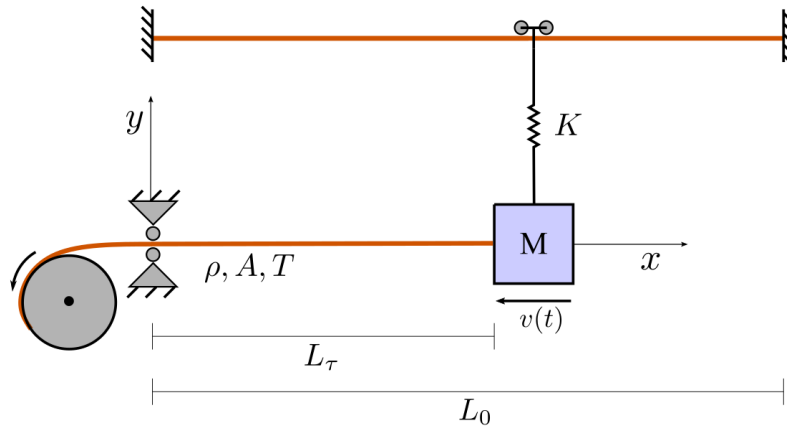


Fig. 2. Schematic representation of the mechanical system used to emulate the aerial cable car system: a variable-length cable coupled to a mass-spring oscillator.

To find the equivalent stiffness of the pair of supporting cables, a simple case study is presented. If one considers the car passing through the extent of the supporting cables to be simplified as a concentrated load F traveling with constant velocity, then the solution of this problem is analytically solved and demonstrated in Hagedorn [8]. In this case the cable deflection is given by

$$w(x, t) = -\frac{2FL_0}{\rho A \pi^2 (c^2 - v^2)} \sum_{j=1}^{\infty} \frac{1}{j^2} \left(\sin \frac{j\pi vt}{L_0} - \frac{v}{c} \sin \frac{j\pi ct}{L_0} \right) \sin \frac{j\pi x}{L_0}, \quad (1)$$

where $c = \sqrt{T/\rho A}$ is a constant having the dimension of speed and the product ρA is the linear density of the cable. Then stiffness can be determined by taking the inverse of the deflection of the supporting cables.

The analytical solution of Eq.(1) is illustrated in Figure 4 for different time instants using the mentioned parameters. It shows the deflection of the cable at different instants while the load moves with velocity v . The parameters used to generate these results are shown in Table 1. The deflection of the rope reaches its maximum value when the load is close to half of the length. Therefore, the rail cable equivalent stiffness value is estimated as

$$K = \frac{F}{w(L_0/2, L_0/2v)}. \quad (2)$$

The following analysis does only concern with the mass being pulled by the cable. We begin by stating the kinetic \mathcal{T} and the potential energy of the rope and the mass. The total kinetic energy is

$$\mathcal{T} = \frac{1}{2} \int_0^{L(t)} \rho [\dot{v}^2 + (\dot{y} + v y')^2] dx + \frac{1}{2} M [\dot{v}^2 + (\dot{y} + v y')^2]_{x=L(t)}, \quad (3)$$

and the total potential energy \mathcal{U} is

$$\mathcal{U} = \frac{1}{2} \int_0^{L(t)} T y'^2 dx + \frac{1}{2} K y^2|_{x=L(t)}. \quad (4)$$

Here, y is the vertical displacement of the moving mass M attached to the pulling cable with linear density ρ and constant traction T . The dot represents the derivation in time and the (') the spatial derivation.

For the traction cable, using the Hamilton principle with the adequate definition of the boundaries conditions and considering the variation of the length gives the following initial-boundary value problem

$$\rho (\ddot{y} + 2v \dot{y} + v^2 y'') = T y'', \quad (5)$$

$$M (\ddot{y} + 2v \dot{y} + v^2 y') + K y = T y' \quad \text{at } x = L(t), \quad (6)$$

$$y = 0 \quad \text{at } x = 0. \quad (7)$$

The first boundary condition, given by Eq.(6), is not homogeneous. This term can be transferred to the differential equation of motion, Eq.(5), by considering

the car's dynamic forces as a concentrated load at $x = L(t)$, rendering a simpler and more intuitive approach [9], given by:

$$\rho(\ddot{y} + 2v\dot{y} + v^2 y'') + 2[M(\dot{y} + 2v\dot{y} + v^2 y' + g) + K y] \delta(x - L(t)) = T y'', \quad (8)$$

$$y = 0 \text{ at } x = 0, \quad (9)$$

$$T y' = 0 \text{ at } x = L(t), \quad (10)$$

where \dot{y} is the time-derivative of y , and y' is the corresponding spatial-derivative with respect to x .

To promote a separation of time scales in the problem, a slow time variation $\tau = \varepsilon t$ is introduced, in which $\varepsilon = v/\omega_0 L_0$, being ω_0 is the natural frequency of the cable without mass and spring, and L_0 the maximum extent of the cable, see [6, 7] for details.

Knowing that $L(t) = L_0 + vt$, so, $v = \dot{L} = \frac{\partial \tau}{\partial t} \frac{\partial L}{\partial \tau} = \varepsilon \nu$, where $\nu = \frac{\partial L}{\partial \tau}$. Therefore, we seek solutions of the form

$$y(x, t) \approx \sum_{i=1}^N \phi_i(x, \tau) q_i(t), \quad (11)$$

where $\phi_i(x, \tau) = \sin(\lambda_\tau^i x)$ and $q_i(t)$ are mode shapes and modal coordinates associated to the underlying eigenvalue problem, respectively. The term λ_τ^i is a slow variation in time of the natural frequency of the cable

$$\lambda_\tau^i = \frac{1}{2} \frac{(2i-1)\pi}{L_\tau}. \quad (12)$$

Applying Eq.(11) into Eq.(8) multiplying by $\phi_j(x, \tau)$ and integrating between 0 and L_τ , it is possible to write the discrete dynamical equation of motion

$$\sum_{i=1}^N [\mathcal{M}_{ij} \ddot{q}_i(t) + \mathcal{G}_{ij} \dot{q}_i(t) + \mathcal{K}_{ij} q_i(t)] = 0, \quad (13)$$

where mass, gyroscopic and stiffness operators components are, respectively, defined by the following expressions

$$\begin{aligned} \mathcal{M}_{ij} &= \int_0^{L_\tau} \rho \phi_i \phi_j dx + M \phi_i(L_\tau) \phi_j(L_\tau) \\ \mathcal{G}_{ij} &= \int_0^{L_\tau} 2\rho \nu \epsilon \phi_i' \phi_j dx + 2M \nu \phi_i'(L_\tau) \phi_j(L_\tau) \\ \mathcal{K}_{ij} &= \int_0^{L_\tau} (\rho \nu^2 \epsilon^2 - T) \phi_i' \phi_j' dx + \\ &\quad \left(M \nu^2 \epsilon^2 \phi_i''(L_\tau) + K \phi_i(L_\tau) \right) \phi_j(L_\tau). \end{aligned} \quad (14)$$

To construct the mass, gyroscopic, and stiffness matrices, the following orthogonality relationships are taken into account

$$\int_0^{L_\tau} \phi_j \phi_i dx = \frac{1}{2} L_\tau \delta_{ij}, \quad \int_0^{L_\tau} \phi_j \phi_i'' dx = -\frac{1}{2} \lambda_i^2 L_\tau \delta_{ij} \quad (15)$$

and that

$$\int_0^{L_\tau} \phi_j \phi_i' dx = -2 \frac{(i-1/2)(j-1/2)}{(i-1/2)^2 - (j-1/2)^2}, \quad (16)$$

where δ_{ij} is the Kronecker delta. As seen in Blevins [10], the result from Eq.(16) exists only when the sum $i+j$ is odd, otherwise it is zero. Also, one has $\phi_i = \sin\left(\frac{1}{2} \frac{(2i-1)\pi}{L_\tau} x\right)$, and $\phi_j = \sin\left(\frac{1}{2} \frac{(2j-1)\pi}{L_\tau} x\right)$.

Thus, for a two-mode approximation ($i = 1..2$ and $j = 1..2$) one gets

$$\begin{aligned} & \left(\frac{1}{2} \rho L_\tau + M\right) \ddot{q}_1(t) - M \ddot{q}_2(t) + \frac{3}{2} \rho \nu \epsilon \dot{q}_2(t) + \\ & \frac{1}{8 L_\tau^2} \left[-2 \pi^2 \epsilon^2 \nu^2 \left(\frac{1}{2} \rho L_\tau + M\right) + L_\tau \pi^2 T + 8 K L_\tau^2 \right] q_1(t) + \\ & \frac{1}{4 L_\tau^2} (M \nu^2 \pi^2 \epsilon^2 - 4 K L_\tau^2) q_2(t) = 0, \end{aligned} \quad (17)$$

$$\begin{aligned} & \left(\frac{1}{2} \rho L_\tau + M\right) \ddot{q}_2(t) - M \ddot{q}_1(t) - \frac{3}{2} \rho \nu \epsilon \dot{q}_1(t) + \frac{1}{4 L_\tau^2} (9 M \nu^2 \pi^2 \epsilon^2 - 4 K L_\tau^2) q_1(t) + \\ & \frac{1}{8 L_\tau^2} \left[-18 \pi^2 \epsilon^2 \nu^2 \left(\frac{1}{2} \rho L_\tau + M\right) + 9 L_\tau \pi^2 T + 8 K L_\tau^2 \right] q_2(t) = 0, \end{aligned} \quad (18)$$

that can be rewritten as

$$\begin{aligned} & \ddot{q}_1(t) - \mu_\tau \ddot{q}_2(t) + \alpha_\tau \dot{q}_2(t) + [(-\beta_\tau - \eta_\tau + \sigma_\tau) + \omega_\tau^2] q_1(t) + \\ & (\eta_\tau - \omega_\tau^2) q_2(t) = 0 \end{aligned} \quad (19)$$

$$\begin{aligned} & \ddot{q}_2(t) - \mu_\tau \ddot{q}_1(t) - \alpha_\tau \dot{q}_1(t) + (9 \eta_\tau - \omega_\tau^2) q_1(t) + \\ & (9(-\beta_\tau - \eta_\tau + \sigma_\tau) + \omega_\tau^2) q_2(t) = 0, \end{aligned} \quad (20)$$

where

$$\begin{aligned} m_\tau &= \frac{1}{2} \rho L_\tau + M, \quad \mu_\tau = \frac{M}{m_\tau}, \quad \alpha_\tau = \frac{3}{2} \frac{\rho \nu}{m_\tau}, \quad \beta_\tau = \frac{\pi^2 \epsilon^2 \nu^2 \rho}{8 L_\tau m_\tau}, \\ \eta_\tau &= \frac{1}{4} \frac{\pi^2 \epsilon^2 \nu^2}{L_\tau^2} \mu_\tau, \quad \sigma_\tau = \frac{\pi^2 T}{8 L_\tau m_\tau}, \quad \text{and } \omega_\tau^2 = \frac{K}{m_\tau}. \end{aligned} \quad (21)$$

The first term, m_τ is the modal mass of the cable along with the cable car mass, which also brings the ratio μ_τ of the masses. The latter couples the system with its acceleration terms. The parameter α_τ represents the Coriolis, and β_τ and η_τ are the centripetal forces of the cable and the mass, respectively. The traction can now be written as σ_τ and the natural frequency from the attached spring as ω_τ . Each of these terms varies in the slow time τ as the pulling cable varies its length.

3 Numerical results and discussion

By inspecting the terms in (21), as well as the Eqs.(19) and (20), it is possible to observe the overall dependency of the cable variation in the slow time τ .

Moreover, some of them are proportional to $\mathcal{O}(1/L_\tau)$ like ω_τ^2 and η_τ ; others are proportional to $\mathcal{O}(1/L_\tau^2)$ like β_τ and σ_τ . It means that β_τ , and σ_τ can become extremely high when the cable length is getting closer to zero. Although, the effect is rather small for η and β_τ , it is usually not for σ_τ . It is worth pointing out that there is a set of values in which σ_τ surpasses the value of ω_τ^2 at a specific length of L_τ .

Table 1. Parameters used to model the rail cable and the traction cable

Supporting Cables			Traction Cable			
Parameter	Value	Unit	Parameter	Symbol	Value	Unit
Linear density	39.20	kg/m	Linear density	ρ	3.83	kg/m
Length	600	m	Initial length	L_0	600	m
Load	32.8	kN	mass	M	6550	kg
Mean Tension	10.0	kN	Mean Tension	T	250	kN
Velocity	6.0	m/s	Stiffness	K	13.4	kN/m

A numerical investigation is conducted and a set of values are given for each of parameters from Eq.(21). Then a simulation of equations (19) and (20) using a 4th and 5th Runge-Kutta solver is done from initial condition of a fully extended length of cable to its almost entire retraction. The parameters used in the simulations match the ones from a real cable car installation, meaning that their values completely feasible and the results may represent the behavior of an actual situation.

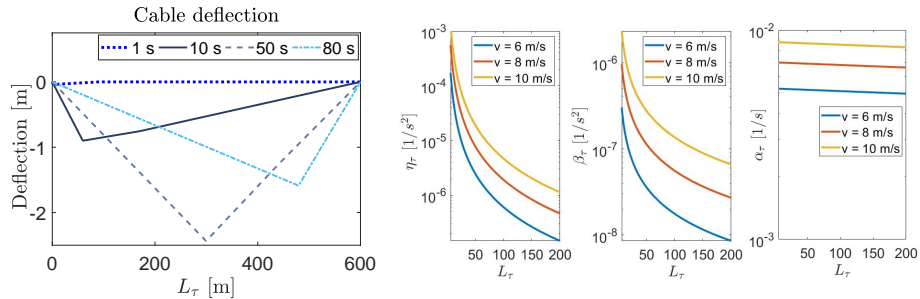


Fig. 3. Parameter variation of the first mode in relation to the length L_τ .

Figure 4 illustrates the variation of the parameters as the traction cable is being retracted by a constant velocity. Three different velocities are tested. Figure 4 shows that the parameters η_τ , β_τ , α_τ have little influence on the overall dynamics, albeit the increase of the travelling speed.

When comparing the parameters σ_τ and ω_τ^2 , one observes in Figure 4a that there is a specific length of the cable that their values are equal, and as the cable car approaches the end, σ_τ becomes even higher that may be relevant to the dynamics. This results in the Fig. 4b where it shows the variation of the natural frequencies as a function of the cable length.

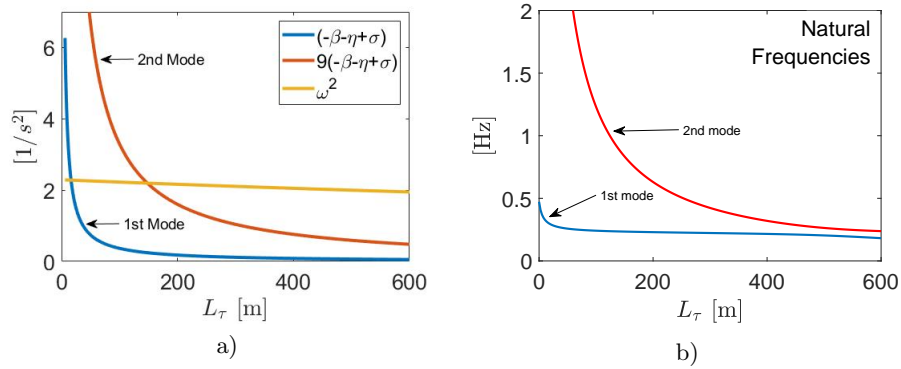


Fig. 4. In (a): The specific length where the natural frequencies depend more of the cable (blue and red) than the rail stiffness (yellow). Travelling speed $v = 6\text{m/s}$. In (b): Variation of the natural frequencies as function of the cable length.

To further investigate the proposed mechanical model a harmonic force is added to the equation presented in section 2 applied to the concentrated mass M . The nature of this force can be seen as an early approximation of the wind mean effect acting directly on the cable-car. A Rayleigh-model damping is also included to emulate the energy dissipation, which also prevents numerical instabilities.

A constant value for the external force frequency is chosen to be $\omega_f = 0.26$ Hz, because it has long period time compatible to the natural behaviour of the wind. Note in Fig. 4b that this becomes the resonance of the system twice as the cable retracts. The result can be seen in Fig. 5, which shows the cable-car displacement time-series $y(t)$. As expected the cable car develops high amplitudes of oscillations twice as the cable gets shorter, and the maximum value of the amplitude gets smaller as the travelling velocity v is higher, due to the shorter period of time that the forcing frequency matches with one of the natural frequencies.

The presence of high amplitude oscillations shown by the numerical simulation is in accordance with the real functioning cable-car seen by the maintenance crew as it approaches the terminal station. These vibrations are mitigated by the breaking system changing the value of the travelling speed v . Also, the model has its own limitations, since by shortening the cable means that the mass M is reaching its boundary condition, which would lead to numerical instabilities or misrepresentation of the real phenomena.

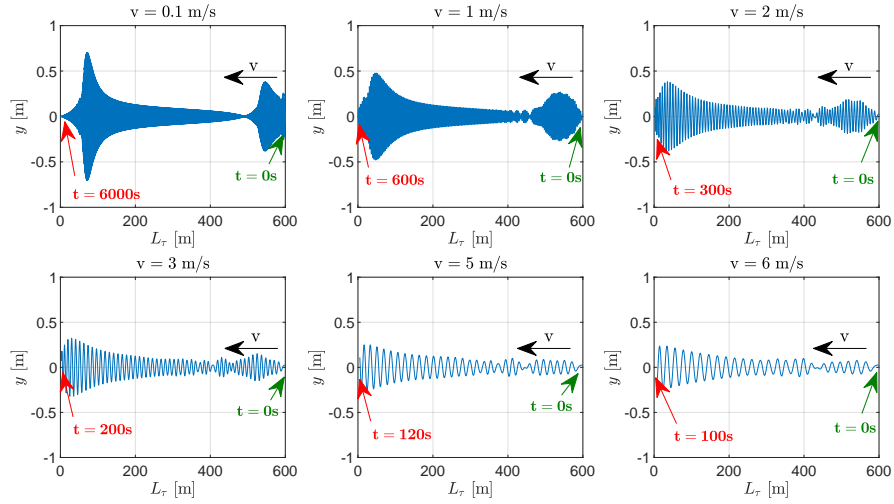


Fig. 5. Displacement for different velocities v of the cable-car when the system is excited by a harmonic force at $F(t) = 300 \sin(\omega_f t)$ [N] at $x = L_r$.

4 Conclusions and future perspectives

This work presented a mechanical-mathematical model for a cable car system. First, the equations of motion are developed, and numerical analysis is conducted with parameters inspired by a real case. This analysis shows the changes of each parameter as a function of the cable length, among them the increase of the stiffness parameter related to the cable.

This paper paves the way for a series of different analysis, which may include the variation of the stiffness parameter related to the pair of supporting cables, the investigation of the influence of a harmonic forcing at the origin, which would represent the machinery responsible for actuating the whole system.

Results show that some points of the trajectory and some speeds present higher amplitude vibrations than others, this is an important non-linear phenomenon that poses challenges to the operation of systems similar to the one modeled. The understanding of those phenomena, as well as its numerical modeling, is of high importance to the safe operation of aerial cable cars.

Another possibility is to include the presence of a random force concentrated at the mass, representing the wind or passengers moving inside the car. Lastly, these models can be compared to other numerical analyses with finite elements models or even with experimental data. This research can also be adapted to other mechanical equivalent found in installations such as in ski lifts.

Acknowledgments

The fourth author would like to thank the financial support given to this research by the Brazilian agencies Coordenação de Aperfeiçoamento de Pessoal de Nível Superior - Brasil (CAPES) - Finance Code 001, and the Carlos Chagas Filho Research Foundation of Rio de Janeiro State (FAPERJ) under the following grants: 211.304/2015, 210.021/2018, 210.167/2019, and 211.037/2019.

References

1. Brownjohn, J.M.W.: Dynamics of an Aerial Cableway System, *Engineering Structures*, Vol. 20, No. 9, pp. 826-836. (1998)
2. Terumichi, Y., Ohtsuka, M., Yoshizawa, M., Fukawa, Y. and Tsujioka, Y.: Nonstationary Vibrations of a String with Time-Varying Length and a Mass-Spring System Attached at the Lower End, *Nonlinear Dynamics*, Vol. 12, pp 39-55. (1997)
3. Bao, J., Zhang, P. and Zhu, C.: Dynamic Analysis of Flexible Hoisting Rope with Time-Varying Length, *International Applied Mechanics*, Vol. 51, No. 6, pp. 710-720. (2015)
4. Kaczmarczyk, S., Iwankiewicz, R.: Dynamic response of an elevator car due to stochastic rail excitation, *Proceedings of the Estonian Academy of Sciences*, Vol. 55, No. 1, pp. 58-67. (2006)
5. Kaczmarczyk, S.: The passage through resonance in a catenary-vertical hoisting cable system with slowly varying length, *Journal of Sound and Vibration*, Vol. 208, No. 2, pp. 243-269. (1997)
6. Cunha Jr.,A., Fonseca, C.A., Rodrigues, G. and Pereira M., Analysis of Vibrations on an Aerial Cable Car System With Moving Mass, *Proceedings of the XV International Symposium on Dynamic Problems of Mechanics, DINAME 2019*, Buzios, RJ, Brazil, March 10th to 15th, 2019
7. Colón,D., Cunha Jr,A., Kaczmarczyk, S., Balthazar, J., On dynamic analysis and control of an elevator system using polynomial chaos and Karhunen-Loève approaches, *Procedia Engineering* 199, pp. 1629–1634 (2017)
8. Hagedorn, P.: *Nonlinear Oscillations*, Oxford Sci. Publ., Oxford. (1988)
9. Meirovitch, L.: *Fundamentals of Vibrations*, McGraw-Hill, New York. (2000)
10. Blevins, R.D.: *Flow-induced Vibration*, Van Nostrand Reinhold, (1990)